Chinese Journal of Structural Chemistry 44 (2025) 100657

Contents lists available at ScienceDirect

Chinese Journal of Structural Chemistry

journal homepage: www.journals.elsevier.com/chinese-journal-of-structural-chemistry

Short Communication

Preparation and characterization of metal carbenes $M_2C_3^-$ (M = Os, Ir, Pt)

Jianpeng Yang [a,*,1], Ziheng Zhang [b,1], Gang Li [b], Juntao Cao [a], Qiangshan Jing [a], Hua Xie [b,**], Ling Jiang [b,c,***]

[a] College of Chemistry and Chemical Engineering, Xinyang Normal University, 237 Nanhu Road, Xinyang, 464000, China
[b] State Key Laboratory of Chemical Reaction Dynamics, Dalian Institute of Chemical Physics, Chinese Academy of Sciences, 457 Zhongshan Road, Dalian, 116023, China
[c] Hefei National Laboratory, Hefei, 230088, China

Transition metals (TMs) are widely recognized for their valuable catalytic properties in various fields, from environmental protection to industrial application [1]. Recently, there has been increasing interest in catalysts containing late TMs, particularly noble metals such as osmium, iridium and platinum. For instance, some studies have demonstrated that the Os atom serves as metal centers that coordinates alkanes, enabling the activation of C–H bonds in the first step [2]. Characterization of the geometric and electronic structures of TM catalysts is essential for exploring the structure-reactivity relationship and elucidating complex mechanisms.

Among numerous TM catalysts, TM carbides have also demonstrated exceptional catalytic performance, attracting considerable attention [3]. In the condensed phase, TM carbides typically exhibit high hardness and/or melting points. In contrast, gas-phase TM carbides serve as ideal models for investigating novel types of catalysts and unraveling the detailed catalytic reaction mechanisms at the molecular level. For example, the quadruple carbides $[V_3C_4]^-$ and $[Ta_2C_4]^-$ facilitate the cleavage of the N≡N bond owing to the robust interactions between the metal core and the empty π* orbitals of N_2 [4]. These studies highlight the critical influence of several factors on the catalytic process, including the identity of metal cores and the geometric/electronic structures of metal carbides, for which these properties can be elucidated by spectroscopic characterization and theoretical calculations [3]. Despite the investigation of numerous late TM carbides, limited information is available regarding the synthesis and chemical properties of the $Os_2C_3^-$, $Ir_2C_3^-$ and $Pt_2C_3^-$ complexes. In this study, we report the generation and photoelectron spectroscopic characterization of these metal carbides (M = Os, Ir, Pt). Combining the experimental results and density functional theory calculations, all the $M_2C_3^-$ (M = Os, Ir, Pt) complexes can be described as the $[MC{=}C{=}C{=}M]^-$ configurations with the delocalized π bonding interactions among all five atoms, featuring the characteristics of metal carbenes with potentially high reactivity toward a series of small molecules. This work not only enhances our understanding of intriguing structures and properties of metal carbenes but also contributes to the exploration and development of novel single-atom/cluster catalysts.

The experimental photoelectron spectra of $M_2C_3^-$ (M = Os, Ir, Pt) were measured by using a homemade photoelectron velocity map imaging analyzer (see Supplementary data for the detailed experimental methods) and are presented in Fig. 1. Generally, the 355 nm spectrum exhibits sharper peaks, while the 266 nm one reveals more spectral features at higher electron binding energy (eBE) regions, because the photons with 266 nm laser have greater capacity for photodetaching inner molecular orbitals (MOs). As exemplified in $Pt_2C_3^-$, only one peak appears in the 355 nm spectrum (Fig. 1(c)), whereas two peaks are observed in the 266 nm spectrum (Fig. 1(f)). This observation highlights the advantage of collecting spectra at different wavelengths and analyzing them together to avoid missing spectral features. The VDE values of $M_2C_3^-$ (M = Os, Ir, Pt) are directly determined from the experimental photoelectron spectra (Fig. 1) to be 2.75 ± 0.09, 3.05 ± 0.08, and 2.06 ± 0.03 eV, respectively, as listed in Table S1 in Supplementary data. The ADE values of $M_2C_3^-$ (M = Os, Ir, Pt) are estimated to be 2.48 ± 0.01, 2.70 ± 0.09, and 1.85 ± 0.04 eV by extrapolating a line to the leading edge of the VDE peak with the consideration of instrumental resolutions.

Based on the experimentally recorded photoelectron spectra, quantum chemical calculations have been performed to elucidate the underlying geometric and electronic structures (see Supplementary data for theoretical methods) and to assist in spectral assignments. For each $M_2C_3^-$ complex, fifteen low-lying isomers were calculated (Figs. S1–S3).

* Corresponding author.
** Corresponding author.
*** Corresponding author. State Key Laboratory of Chemical Reaction Dynamics, Dalian Institute of Chemical Physics, Chinese Academy of Sciences, 457 Zhongshan Road, Dalian, 116023, China.
E-mail addresses: yangjpchem@126.com (J. Yang), xiehua@dicp.ac.cn (H. Xie), ljiang@dicp.ac.cn (L. Jiang).
[1] Authors contributed equally.

https://doi.org/10.1016/j.cjsc.2025.100657
Received 29 April 2025; Received in revised form 25 June 2025; Accepted 25 June 2025
Available online 27 June 2025

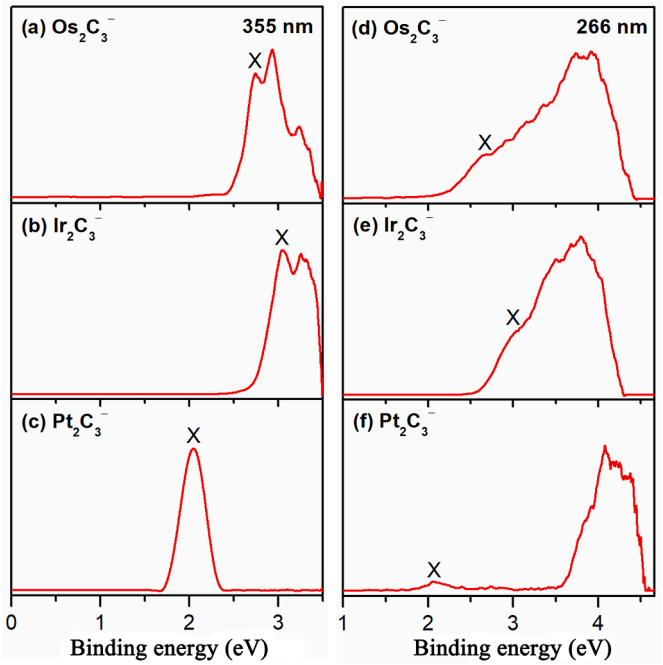

Fig. 1. Photoelectron spectra of $M_2C_3^-$ (M = Os, Ir, Pt) at 355 nm (a–c) and 266 nm (d–f).

According to Boltzmann distribution, only the four lowest-energy isomers (Fig. 2) were considered for further ADE/VDE value calculations and spectral simulations (A vibrational temperature of 150 K was assumed for the anion in the simulation). Table S1 compares the calculated relative energies, ADE, and VDE values of these four isomers at the B3LYP/aug-cc-pVTZ-PP (M = Os, Ir, Pt)/aug-cc-pVTZ (C) level of theory.

The calculated VDE/ADE values of 2.61/2.46, 2.95/2.75, and 2.15/1.85 eV for the lowest-lying isomers 3A, 3a, and 3-I are in excellent agreement with the corresponding experimental values of 2.75/2.48, 3.05/2.70, and 2.06/1.85 eV (Table S1), respectively. As shown in Fig. S4, the simulated density of states (DOS) spectra closely replicate the experimental spectral contours, further confirming the presence of these lowest-lying isomers. The energetically higher isomers 3B−3D, 3b−3d, and 3-II−3-IV could be ruled out by their discrepancies of simulated ADE/VDE values (Table S1) and simulated spectral patterns (Fig. S4) from the experimental values. We also calculated the 3A, 3a and 3-I structures with the CCSD(T)/aug-cc-pVTZ-PP (M = Os, Ir, Pt)/aug-cc-pVTZ (C) method and the results are given in Table S2. The VDE values of the most stable isomers 3A, 3a and 3-I calculated at the CCSD(T)/aug-cc-pVTZ-PP (M = Os, Ir, Pt)/aug-cc-pVTZ (C) level are

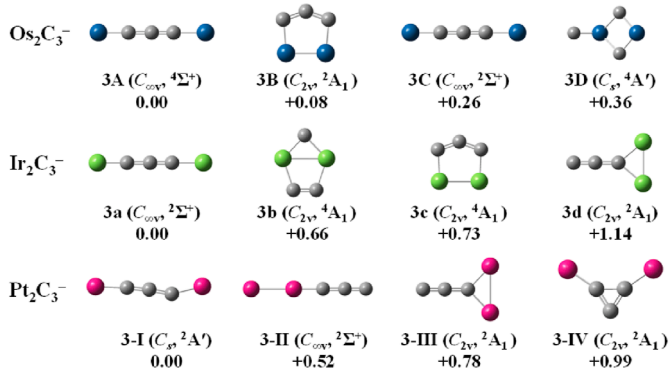

Fig. 2. Optimized structures of the lowest-energy isomers for $M_2C_3^-$ (M = Os, Ir, Pt) calculated at the B3LYP/aug-cc-pVTZ-PP (M = Os, Ir, Pt)/aug-cc-pVTZ (C) level. Relative energies are given in eV.

4.62, 4.75, and 2.01 eV, respectively, and the VDE results of 3A and 3a are not consistent with the experimental values.

As shown in Fig. 2, the most stable structure of $Os_2C_3^-$ (isomer 3A) adopts a linear chain "Os–C–C–C–Os" geometry with $C_{\infty v}$ symmetry and a $^4\Sigma^+$ electronic state. Analogous to isomer 3A, the 3a isomer for $Ir_2C_3^-$ also features a linear chain "Ir–C–C–C–Ir" geometry with $C_{\infty v}$ symmetry and a $^2\Sigma^+$ electronic state. The 3-I isomer for $Pt_2C_3^-$ shows a slightly distorted zigzag geometry with C_s symmetry and a $^2A'$ electronic state. It could be rationalized by the structural transformation during the photodetachment process of $Pt_2C_3^-$. To corroborate this hypothesis, we calculated the structure of the neutral Pt_2C_3 (singlet) as shown in Fig. S5. Notably, the neutral Pt_2C_3 adopts a linear-chain structure, which is distinctly different from the zigzag configuration of the $Pt_2C_3^-$ anion. Nevertheless, all the $M_2C_3^-$ (M = Os, Ir, Pt) anions share a common structural feature of a chain structure, rather than ring or three-dimensional structures.

The $Os_2C_3^-$ and $Ir_2C_3^-$ complexes exhibit linear-chain structures, which also exist in the metal carbide $Rh_2C_3^+$ of the same VIII family in periodic table [5]. The $Pt_2C_3^-$ carbide has a lower symmetry (C_s) of zigzag structure, which is slightly different from the structures of $Os_2C_3^-$ and $Ir_2C_3^-$. The structural difference between the most stable isomer of anionic $Pt_2C_3^-$ (slightly bent zigzag) and neutral Pt_2C_3 (linear geometry) is stemmed from electronic transitions. It is noteworthy that $Pt_2C_3^-$ bears a structural resemblance to $[O_2C_3]^-$ [6]. This similarity aligns with findings from our previous study, which revealed a "strikingly" structural and bonding resemblance between PtC_3 and OC_3 clusters [7]. The $[O_2C_3]^-$ anion has been demonstrated to undergo a considerably geometric change during the photodetachment process [8], which characteristics bear striking similarities to $Pt_2C_3^-$. Moreover, the carbon chains display remarkable C–C bond length alternation with the short C–C bonds about 1.26 Å and long C–C bonds about 1.32 Å, suggesting a conjugated double bond character, and the metal-C bonds are all double bonds. In consequence, the $M_2C_3^-$ (M = Os, Ir, Pt) complexes can be identified to have the $[M{=}C{=}C{=}C{=}M]^-$ configurations. The binding energies between MC_3^- and M (M = Os, Ir, Pt) are calculated to be 3.39, 3.21, and 1.99 eV, respectively, indicating that the formation of $M_2C_3^-$ is highly exothermic and kinetically feasible in the gas phase. These results reveal the strong interaction between metal and C atoms as well as the thermodynamic stability of these structures.

Fig. S6 shows the frontier canonical Kohn-Sham MOs of $M_2C_3^-$ (M = Os, Ir, Pt). These three complexes are found to exhibit similar chemical bonding characteristics. Here, we take $Os_2C_3^-$ as an example to discuss the bonding schemes. $Os_2C_3^-$ possesses three singly occupied molecular orbitals (SOMOs), among which the doubly degenerate SOMO represents the C–C π bonding and metal–C π* anti-bonding orbitals. The doubly degenerate HOMO-3 of $Os_2C_3^-$ has metal–C π bonding and C–C π* anti-bonding orbitals. The doubly degenerate HOMO-4 of $Os_2C_3^-$ exhibits typical delocalized π bonding interactions between the C–C and metal–C atoms, while SOMO-1 and HOMO-1 represent σ-type metal–C bonding. This bonding analysis suggests that each bond in $Os_2C_3^-$ consists of one σ and one π bonds. Since no significant vibrational discrimination is observed in the experimental spectra, it is difficult to assign each peak to the corresponding neutral species. According to the results in Fig. S6, for $Os_2C_3^-$ and $Ir_2C_3^-$, the electron is detached from the metal atom, corresponding to the SOMO-2 and SOMO orbitals, respectively; the electron of $Pt_2C_3^-$ is detached from the SOMO orbital of the entire complex. To further explore the chemical bonding in the $M_2C_3^-$ (M = Os, Ir, Pt) complexes, the adaptive natural density partitioning (AdNDP) has been performed at the B3LYP/aug-cc-pVTZ/ECP level of theory, as shown in Fig. S7–9. AdNDP analyses reveal the same bonding characteristics between the M and C atoms in the most stable isomers 3A, 3a and 3-I, which indicate strong interaction among these atoms and the stability of the structures for $M_2C_3^-$ (M = Os, Ir, Pt) complexes.

The isosurface maps of unpaired spin density distributions for $M_2C_3^-$ (M = Os, Ir, Pt) (Fig. S10) reveal that the spin density on the metal atom gradually decreases with the increase of atomic number. The

contributions of unpaired spin density distribution for Os, Ir and Pt in $M_2C_3^-$ (M = Os, Ir, Pt) are summarized in Table S3. The calculated values for spin contamination ($<S^2>$) of $Os_2C_3^-$ (quartet), $Ir_2C_3^-$ (doublet), and $Pt_2C_3^-$ (doublet) are 3.824, 0.766 and 0.774, respectively. Note that the expectation values of spin contamination for a doublet and quartet states are 0.75 and 3.75, respectively. Then, the deviations of calculated value from the expectated value for spin contamination of $Os_2C_3^-$ (quartet), $Ir_2C_3^-$ (doublet), and $Pt_2C_3^-$ (doublet) are 0.074, 0.016, and 0.024, respectively, which are all less than 0.1. Accordingly, these calculated values for spin contamination of $Os_2C_3^-$, $Ir_2C_3^-$, and $Pt_2C_3^-$ indicate a negligible loss in accuracy for the present B3LYP/aug-cc-pVTZ-PP (M = Os, Ir, Pt)/aug-cc-pVTZ (C) calculations. In $Os_2C_3^-$ and $Ir_2C_3^-$, the spin density is predominantly localized on Os (3.16) and Ir (1.02), with a 100% contribution from their 5d orbitals. In contrast, for $Pt_2C_3^-$, the spin density on Pt is relatively low (0.38), with contribution from the 6s, 6p and 5d orbitals at 9%, 46%, and 45%, respectively. As shown in Fig. 2, the most stable structure of $Os_2C_3^-$ has a quartet electronic state with three single electrons; while the most stable structure of $Ir_2C_3^-$ has a doublet electronic state with only one single electron, indicating that the spin densities are asymmetric, consistent with the calculated results in Table S3. The varying distributions of spin densities result in different bonding modes for the M–C bonds. This is reflected in the bond lengths and Wiberg bond orders of the M−C bonds, as shown in Table S4. Consequently, $M_2C_3^-$ (M = Os, Ir, Pt) feature metal carbenes, which may enable high reactivity in many important reactions (i.e., N–N activation, C–O activation, C–C coupling) [1]. The reactivity and reaction pathways of some heteronuclear metals and their oxides with small molecules such as CO and N_2 have been recently discussed [9].

In summary, the $M_2C_3^-$ (M = Os, Ir, Pt) complexes have been successfully synthesized and characterized by using photoelectron spectroscopy. The experimental VDEs of $Os_2C_3^-$, $Ir_2C_3^-$ and $Pt_2C_3^-$ are measured to be 2.75 ± 0.09, 3.05 ± 0.08, and 2.06 ± 0.03 eV, respectively, all in remarkable consistency with the theoretical values obtained from quantum chemical calculations. While the structures of $Os_2C_3^-$ and $Ir_2C_3^-$ have linear chains with two terminal metal atoms, $Pt_2C_3^-$ adopts a slightly twisted zigzag chain. All the $M_2C_3^-$ (M = Os, Ir, Pt) complexes are stabilized by the delocalized π bonding interactions among all the five atoms, indicative of a $[M{=}C{=}C{=}C{=}M]^-$ carbene with potentially high reactivity toward a large variety of small molecules (CO_2, N_2, H_2O, CH_4, etc). The present findings advance the characterization of novel metal carbenes and afford important insights into the development of related single-atom/cluster catalysts.

CRediT authorship contribution statement

Jianpeng Yang: Writing – review & editing, Writing – original draft, Investigation, Formal analysis, Data curation, Conceptualization. **Ziheng Zhang:** Software, Investigation, Formal analysis, Data curation. **Gang Li:** Validation, Resources, Methodology. **Juntao Cao:** Validation, Software, Resources. **Qiangshan Jing:** Software, Resources, Methodology. **Hua Xie:** Writing – review & editing, Writing – original draft, Supervision, Project administration, Funding acquisition, Conceptualization. **Ling Jiang:** Writing – review & editing, Writing – original draft, Supervision, Project administration, Funding acquisition, Conceptualization.

Declaration of competing interest

The authors declare no competing interests.

Acknowledgements

The authors gratefully acknowledge the staff members of the Dalian Coherent Light Source (31127.02.DCLS) for technical support and assistance in data collection. This work was supported by the National Natural Science Foundation of China (22273101, 22125303, 92361302, 22373102, 21327901, and 22288201), the Youth Innovation Promotion Association of the Chinese Academy of Sciences (2020187), the Innovation Program for Quantum Science and Technology (2021Z D0303304), the International Partnership Program of the Chinese Academy of Sciences (121421KYSB20170012), the Scientific Instrument Developing Project of the Chinese Academy of Sciences (GJJS TD20220001), and Dalian Institute of Chemical Physics (DICP I202437).

Appendix A. Supplementary data

Supplementary data to this article can be found online at https://doi.org/10.1016/j.cjsc.2025.100657.

References

[1] B. Qiao, A. Wang, X. Yang, L.F. Allard, Z. Jiang, Y. Cui, J. Liu, J. Li, T. Zhang, Single-atom catalysis of CO oxidation using Pt_1/FeO_x, Nat. Chem. 3 (2011) 634–641.
[2] S. Li, X.-N. Wu, S. Zhou, Methane activation by $[OsC_3]^+$: implications for catalyst design, J. Phys. Chem. Lett. 14 (2023) 5236–5240.
[3] C. Geng, T. Weiske, J. Li, S. Shaik, H. Schwarz, Intrinsic reactivity of diatomic 3d transition-metal carbides in the thermal activation of methane: striking electronic structure effects, J. Am. Chem. Soc. 141 (2019) 599–610.
[4] Z.-Y. Li, Y. Li, L.-H. Mou, J.-J. Chen, Q.-Y. Liu, S.-G. He, H. Chen, A facile N≡N bond cleavage by the trinuclear metal center in vanadium carbide cluster anions $V_3C_4^-$, J. Am. Chem. Soc. 142 (2020) 10747–10754.
[5] H.C. Wu, X.-N. Wu, X.Y. Jin, Y.Y. Zhou, W. Li, C.L. Ji, M.F. Zhou, Quadruple C–H bond activations of methane by dinuclear rhodium carbide cation $[Rh_2C_3]^+$, JACS Au 1 (2021) 1631–1638.
[6] L. Wang, S. Pan, B. Lu, X. Dong, H. Li, G. Deng, X. Zeng, M. Zhou, G. Frenking, Generation and characterization of the $C_3O_2^-$ anion with an unexpected unsymmetrical structure, Angew. Chem. Int. Ed. 60 (2021) 4518–4523.
[7] X. Liu, G. Li, Z. Liu, W. Yang, H. Fan, L. Jiang, H. Xie, Isoelectronic IrC_3^-, PtC_3, and AuC_3^+ clusters featuring the structural and bonding resemblance to OC_3, J. Phys. Chem. Lett. 13 (2022) 12–17.
[8] S. Feng, Z. Li, W. Liu, Q. Zhang, Y. Chen, D. Zhao, Photoelectron spectroscopy confirms the gas-phase stability of the $C_3O_2^-$ anion, J. Phys. Chem. Lett. 14 (2023) 8599–8603.
[9] J. Zhang, Z. Zhang, G. Li, H. Qiao, H. Xie, L. Jiang, Ligand-mediated reactivity in CO oxidation of yttrium-nickel monoxide carbonyl complexes, Chin. Chem. Lett. 36 (2025) 110278.